The point-to-point uncertainty on the centre-of-mass energy and the Z width at FCC-ee

Emmanuel Perez

CERN, EP Department, Geneva, Switzerland.
Emmanuel.Perez@cern.ch.

Abstract

The Tera-Z run at the FCC-ee, with a total of about $\mathbf{6 \times 10^{12}}$ Z bosons produced, offers the potential for electroweak measurements at an unprecedented level of accuracy. That is the case in particular for the Z width, which would be extracted from the Z lineshape scan with a statistical uncertainty of 4 keV. One of the leading sources of systematic uncertainty for this measurement is expected to be the relative, point-to-point uncertainty of the measurement of the centre-of-mass energy ($\sqrt{s}$), namely the uncertainty of the difference between the energies at which the machine will run for the lineshape scan. For the corresponding systematic uncertainty on the Z width to be commensurate with the statistical uncertainty, this difference will have to be known to much better than what will be derived from the absolute measurements of $\sqrt{s}$ resulting from the resonant depolarisation method. This note explores the potential for controlling this systematic uncertainty in-situ using dimuon events. An excellent track momentum resolution is a key requirement for the proposed method.

1 Introduction

The context of the study reported in this note is the extraction of the width of the Z boson from the Z lineshape scan, as could be performed at the FCC-ee collider. The width of the Z, Γ_{Z}, together with its mass m_{Z} and the hadronic Z production cross-section at the peak, is extracted from a fit of the Z production cross-sections measured at the Z peak and at a few off-peak values of the centre-of-mass energy $\sqrt{s}$. The current baseline scenario for the "Tera-Z" run of FCC-ee is to collect data at $\sqrt{s}_0 = 91.2$ GeV, at $\sqrt{s}_- = 87.9$ GeV and at $\sqrt{s}_+ = 94.3$ GeV, at four interaction points, for a total integrated luminosity of 125 ab^{-1} at the peak, and of 40 ab^{-1} for each off-peak point. With this statistics, the mass and the width of the Z boson can be determined with an unprecedented statistical uncertainty of 4 keV and these measurements will be systematically limited. It is crucial, though, to understand how these systematic uncertainties can be reduced and made commensurate with the statistical uncertainty. The measurement of the Z mass is limited by the absolute calibration of the centre-of-mass energy, which will be known to better than 100 keV thanks to the resonant depolarisation (RDP) method [1]. In contrast, for the measurement of the Z width, what matters is the relative uncertainty of $\sqrt{s}$ between the different energy points used in the scan, namely the knowledge of the difference $\sqrt{s_+} - \sqrt{s_-}$. Would this point-to-point uncertainty on the centre-of-mass energy, $\delta_{\mathrm{ptp}}(\sqrt{s})$, be controlled to 10 keV, the corresponding systematic uncertainty on Γ_Z would be equal to the statistical uncertainty. As will be shown in this note, $\delta_{\mathrm{ptp}}(\sqrt{s})$ can be determined in-situ using dimuon events, with a much better precision than what would result from the RDP measurements of $\sqrt{s}$ at the different energies, namely $\sim \sqrt{2} \times 100$ keV.

2 In-situ determination of $\sqrt{s}$ from dimuon events

2.1 Overview of the method

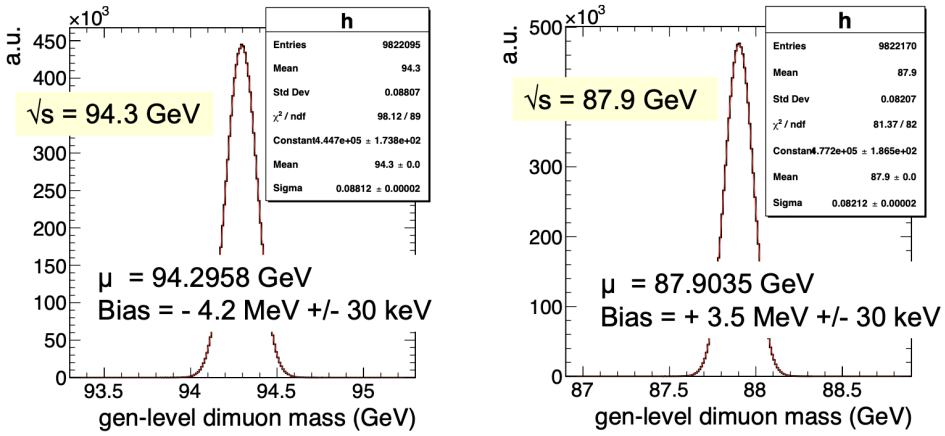

Fig. 1: Distribution of the invariant mass of the muon pair at the generator-level, in a Monte-Carlo simulation of about 10^7 events where QED radiation effects have been disabled, at $\sqrt{s} = 94.3$ GeV (left) and $\sqrt{s} = 87.9$ GeV (right). The result of a fit with a simple Gaussian function is overlaid.

The potential of dimuon events at FCC-ee for in-situ "beam diagnostics" has been pioneered in Ref. [1], where it is shown that the crossing angle of the two beams at the interaction point, and the beam energy spread (whose knowledge is also crucial for the extraction of Γ_Z) can be determined very precisely from the large statistics of $e^+e^- \to \mu^+\mu^-(\gamma)$ events, whose kinematics is fully constrained by the conservation of energy-momentum. In the same paper, it was also proposed to use the distribution of the invariant mass of such dimuon events, M, to measure directly the centre-of-mass energy: the position of the peak of this distribution is a possible proxy for the centre-of-mass energy. Due to the large effect of QED radiations, it may not be good enough for an absolute calibration of $\sqrt{s}$, but the difference between the peak positions seen at two energies may provide the difference between the two values of $\sqrt{s}$ with a good precision. The key for a precise determination of the peak position of the M distribution is the track momentum resolution. With the very light drift chamber of the IDEA detector concept [2], the latter amounts to about 0.15% for 45 GeV central muons, and is typically worse by a factor of two with the heavier silicon tracker of the CLD detector [3], due to the large amount of multiple scattering.

However, any proxy of the centre-of-mass energy, be it the peak position of the M distribution, or some parameter related to it that would be extracted from a fit, is likely to show a bias that has to be corrected for. In particular, in view of the determination of $\delta_{\rm ptp}(\sqrt{s})$, the dependence of this bias with $\sqrt{s}$ must be understood. As illustrated in Fig. 1, this bias is not only due to QED radiative effects. The figure shows the distribution of the generator-level dimuon mass at $\sqrt{s} = 94.3$ GeV and at $\sqrt{s} = 87.9$ GeV, in a Monte-Carlo simulation of $e^+e^- \to \mu^+\mu^-$ events where the effects of initial state radiation (ISR) and final state radiation (FSR) have been switched off. The peak position is obtained from a fit to these distributions with a simple Gaussian. The mean of the fitted Gaussian underestimates the true value of the centre-of-mass energy by about 4 MeV at $\sqrt{s} = 94.3$ GeV, and it overestimates it by about 3.5 MeV at $\sqrt{s} = 87.9$ GeV. This bias results from the product of the Breit-Wigner that describes the Z resonance with the Gaussian function that represents the beam energy spread (BES). When the centre-of-mass energy is lower than the Z mass, the Breit-Wigner "pulls" the distribution towards $M_{\rm Z}$, leading to a positive bias, while the opposite happens when $\sqrt{s}$ is above the Z mass. The value of this bias can be determined analytically, by finding the value of x that maximises the product of the Breit-Wigner with

a Gaussian:

$$f(x) = \exp\left(-\frac{1}{2}\left(\frac{\mathrm{x}-\sqrt{\mathrm{s}}}{\sigma}\right)^2\right) \times \frac{\mathrm{M_Z^2}}{(\mathrm{x}^2-\mathrm{M_Z^2})^2+\mathrm{M_Z^2}\Gamma_\mathrm{Z}^2} \tag{1}$$

or, using the energy-dependent expression of the Breit-Wigner:

$$f(x) = \exp\left(-\frac{1}{2}\left(\frac{\mathrm{x}-\sqrt{\mathrm{s}}}{\sigma}\right)^2\right) \times \frac{\mathrm{x}^2}{(\mathrm{x}^2-\mathrm{M_Z^2})^2+\mathrm{x}^4\Gamma_\mathrm{Z}^2/\mathrm{M_Z^2}} \tag{2}$$

Using a relative beam energy spread of 0.132%, i.e. $\sigma = \frac{0.132\%}{\sqrt{2}} \times \sqrt{s}$ in the equations above, the bias obtained from this maximisation is shown in Fig. 2 as a function of the centre-of-mass energy. The resulting bias does not depend much on the description of the Breit-Wigner. This analytic determination is in very good agreement with the biases determined from fits to the dimuon mass distribution of Monte-Carlo events illustrated in Fig. 1. The analytic determination also shows that the bias scales quadratically with the beam energy spread.

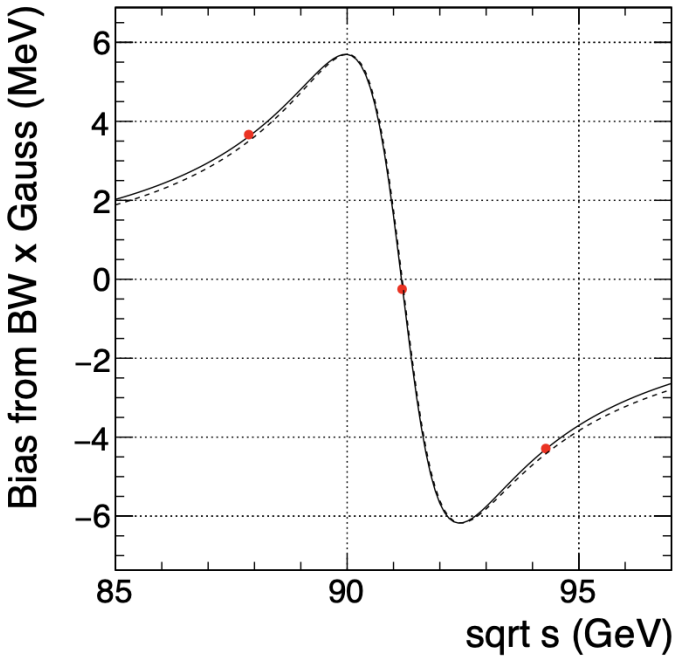

Fig. 2: Difference between the value that maximises the function given in Equation 1 (full curve) or Equation 2 (dashed curve) and the value of $\sqrt{s}$, as a function of $\sqrt{s}$. The red symbols show the bias obtained from Gaussian fits as depicted in Fig. 1 using Monte-Carlo simulations with no ISR and FSR.

2.2 Description of the fit procedure

The Monte-Carlo samples used for this study have been produced with the `KKMC` [4] and the `Whizard v3.0.3` [5] programs, taking into account the beam energy spread as well as initial and final state radiation. The events were passed through a fast simulation of the IDEA or of the CLD detector using the `DELPHES` package [6]. Samples have been produced at the nominal energies $\sqrt{s_0}$, $\sqrt{s_+}$ and $\sqrt{s_-}$, and, for test purposes, at a few other off-peak energies. Each sample consists of 100 millions events.

At each energy, fits to the dimuon mass distribution are made, from which an estimator of the centre-of-mass energy is extracted. The distribution of the "raw" dimuon invariant

mass is used, i.e. no attempt is made to account for a potential radiated photon. Following the studies reported in Ref. [7], the fit model consists of the sum of a Gaussian function with the convolution of this Gaussian with two exponentials that describe the effects of QED radiations. Compared to an alternative choice where the Gaussian function would be replaced by the product of a Gaussian with a Breit-Wigner, this function has the advantage that the convolution is analytically integrable. It provides indeed good fits to the mass distributions for the Monte-Carlo statistics used here, as will be shown below. To account for the angular dependence of the track momentum resolution, the fits are done in bins of polar angle[1]. A collinearity cut is applied, that requires that $\theta^+ - (\pi - \theta^-) < 0.1\,\text{rad}$ where $\theta^\pm$ denote the polar angle of the $\mu^\pm$, and the events are binned according to the average $0.5 \times (\theta^+ + (\pi - \theta^-))$. In each angular bin, a likelihood fit to the M distribution is made using the `RooFit` package [8]. The upper range of the fit is set to the nominal value of $\sqrt{s}$ plus a few hundreds of MeV (the exact value depending on the resolution). The lower range of the fit is dynamic and determined separately for each fit: starting from a low value, this lower bound is increased in steps of 100 MeV, and the value for which the fit leads to the best description of the simulated data is chosen. Potential bad fits, based on the χ^2 between the actual distribution and the fit result, are not considered further.

The proxy for $\sqrt{s}$ is obtained by averaging the mean of the fitted Gaussian ($\hat{\mu}$) across the various angular bins in which good fits have been obtained. A simple iterative procedure that removes potential "outlier" fits is applied. The weighted average of the $\hat{\mu}$'s resulting from all good fits is first obtained. The bin for which the fitted $\hat{\mu}$ shows the largest deviation with this average is identified, and if this deviation is larger than three times the uncertainty of $\hat{\mu}$, this bin is removed and a new average is calculated. The procedure is iterated until no outlier remains (in practice, such outliers are not frequent), and the weighted average of $\hat{\mu}$ in the bins that survive the outlier removal procedure, $< \hat{\mu} >$, defines the proxy for $\sqrt{s}$.

Figure 3 illustrates the fit procedure using the dimuon invariant mass at the generator level and the sample at $\sqrt{s} = 94.3$ GeV. The top-left panel shows the mass distribution in an example bin in the central region of the detector, together with the result of the fit and its various components; the corresponding pulls are shown in the top-right panel. The bottom plots show the mean and the σ of the fitted Gaussian in the various bins of polar angle (each point corresponds to one fit made in a given bin), the left part of each plot corresponding to the central region of the detector, the right part to the forward/backward region. Within the uncertainties, the parameters of the fitted Gaussian are the same in all bins, and the weighted average is shown by the red line. Moreover, the fitted σ is close to what is expected from the beam energy spread.

Figure 4 shows a similar sets of plots, again at $\sqrt{s} = 94.3$ GeV, but using the reconstructed dimuon mass in the IDEA detector. The bottom-left panel illustrates the aforementioned procedure that removes "outlier" fits: in one bin (shown by the black symbol), the mean of the fitted Gaussian is inconsistent with the average in the other bins, and this fit is excluded when determining the average $< \hat{\mu} >$ that defines the proxy for $\sqrt{s}$. As shown in the bottom-right panel, the fitted σ of the Gaussian now shows a dependence with the angular bin. Moving from the centre of the detector (leftmost part of the plot) to the forward or backward region (rightmost part of the plot), the track momentum resolution first improves slightly since the overall transverse momentum of the $p \simeq 45$ GeV muons decreases, until the point where the multiple scattering induced by the larger material in the forward region becomes significant, leading to an increase of the fitted σ.
The case of the CLD detecor is illustrated in Fig. 5 for $\sqrt{s} = 87.9$ GeV. The fitted σ of the Gaussian is significantly larger than in the IDEA case in particular in the forward angular bins, reflecting the much larger amount of material of a pure silicon tracker compared to a gaseous detector, and the resulting degradation of the resolution due to multiple scattering.

[1]The polar angle, θ, is defined with respect to the direction of the electron beam, and takes values between zero and π radians. In the simulations used here, the electron and positron beams collide head-on. This technical simplification is justified since, after unfolding the transverse boost of the final state particles that arises from the non-vanishing crossing-angle of the beams at FCC-ee, the head-on situation is recovered.

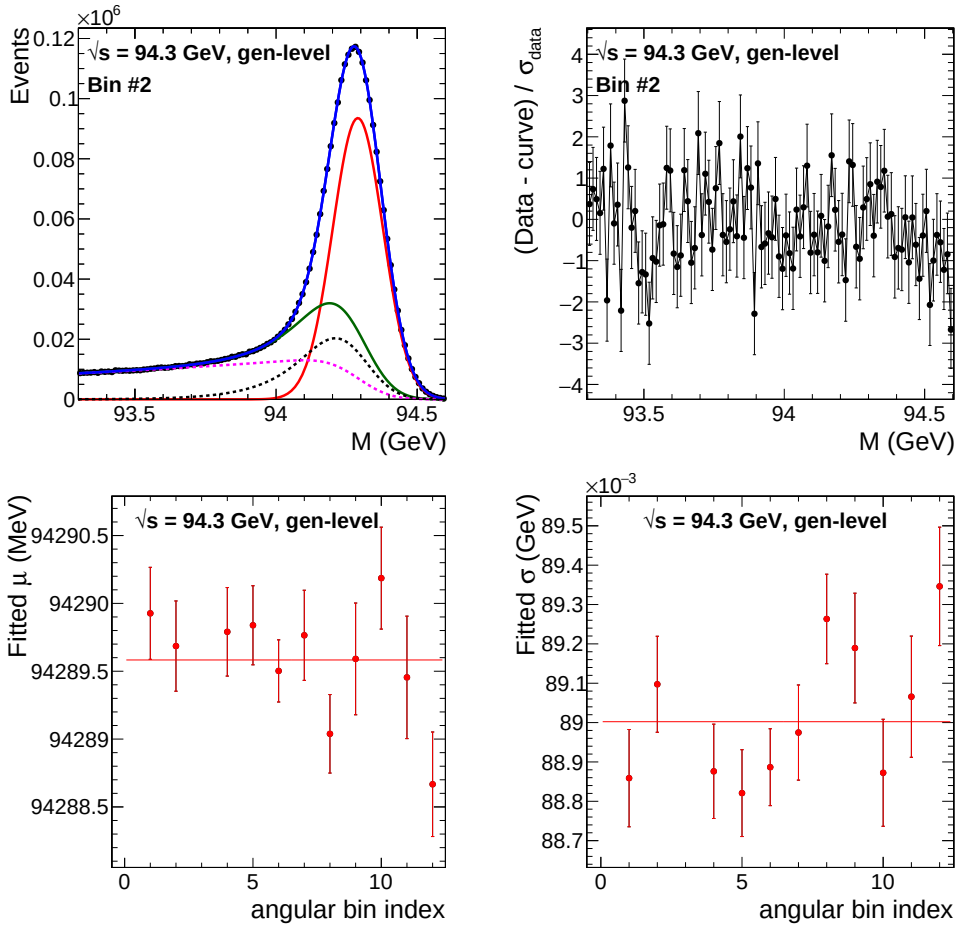

Fig. 3: Top row: example fit of the distribution of the dimuon invariant mass at the generator level (left) together with the corresponding pulls (right), at $\sqrt{s} = 94.3$ GeV. The fit shown here corresponds to rather central events, where one of the muons is emitted at a polar angle around 75 degrees. In the left panel, the symbols represent the simulated data and the full blue curve shows the result of the fit. The red curve shows the Gaussian core of the fitted function, while the dashed black and magenta curves show the convolution of this Gaussian with the two exponential functions used in the model; the full green curve is the sum of the two dashed curves. Bottom row: the mean (left) and width (right) of the Gaussian function of the fit model, resulting from fits in the various bins in polar angle. The leftmost (rightmost) part of the plots, with small (large) values of the bin index, corresponds to the central (forward/backward) part of the detector.

2.3 Determination of $\sqrt{s_+} - \sqrt{s_-}$ and its uncertainty

By definition, the bias b of the determination of the centre-of-mass energy from the aforementioned proxy is equal to

$$b \quad = \quad < \hat{\mu} > \quad - \sqrt{s} \tag{3}$$

such that the difference between the two off-peak centre-of-mass energies can be written as

$$\sqrt{s_+} - \sqrt{s_-} \; = \; \left(\quad < \hat{\mu}(\sqrt{s_+}) > - < \hat{\mu}(\sqrt{s_-}) > \quad \right) \; - \; \left(\quad b(\sqrt{s_+}) - b(\sqrt{s_-}) \quad \right) \tag{4}$$

The first term is the difference between the proxies measured at the two energies. With 10^8 events, the statistical uncertainty of $< \hat{\mu} >$ amounts to about 200 keV at $\sqrt{s_0}$ and $\sqrt{s_-}$, and to about 300 keV at $\sqrt{s_+}$, with the resolution of the IDEA detector. Within these uncertainties, the values of $< \hat{\mu} >$ determined from the `Whizard` and the `KKMC` Monte-Carlo samples are in very good agreement. The uncertainty is a bit higher at $\sqrt{s}_+$ because the

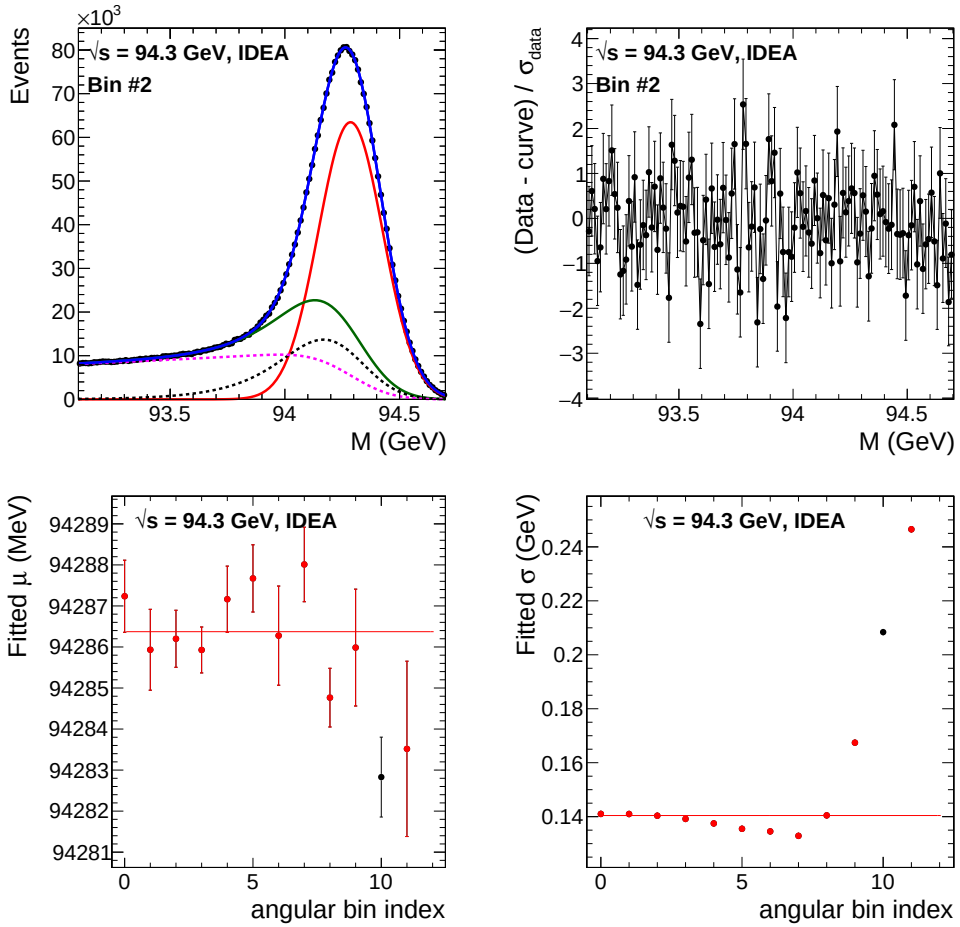

Fig. 4: Same as Figure 3, but using the reconstructed mass in the IDEA detector. In the bottom left plot, the value of the μ parameter resulting from the fit in bin number 10 (black symbol) is inconsistent with the average across the other bins (red symbols), and this fit is excluded when determining the average $< \hat{\mu} >$ that defines the proxy for $\sqrt{s}$. The red line shows this latter average.

energy range over which the exponential component of the fit function is constrained can be reduced compared to what it is at and below the Z peak. This effect is due to radiative-return events that cause a "bump" in the mass distribution, and it gets more pronounced in the forward angular bins, where the experimental resolution worsens. From a rescaling of these uncertainties to the number of events expected with the full FCC-ee luminosity, the proxy for $\sqrt{s}$ will be known to 4 keV at 91.2 GeV, and to about 20 keV for the two off-peak energies. With the resolution of the CLD detector, these uncertainties are larger, by about 50% at and below the Z peak, and by a factor of two at $\sqrt{s_+}$. Figure 6 summarises the statistical uncertainties with which $< \hat{\mu} >$ can be determined at the three energies, with the resolution of both detectors, and assuming an ideal experimental resolution. With the IDEA resolution, the first term in Eq. 4 will thus be known to $20 \oplus 20 = 28$ keV.

The second term in Eq. 4 is the difference, Δb, between the biases expected at the two energies. This term has to be taken from Monte-Carlo predictions. It is thus crucial to understand the accuracy at which the QED radiation effects and the detector response must be modelled, in order to ensure that the systematic uncertainty on Δb is smaller than this 28 keV.

The dependence of the bias with the centre-of-mass energy, obtained from fitting the Monte-Carlo samples modelling the IDEA detector response at $\sqrt{s_0}$, at $\sqrt{s_\pm}$ and at a few additional energy points, is shown in the left panel of Fig. 7. The shape is very similar to that of Fig. 2, suggesting that most of the dependence is coming from the interplay of the

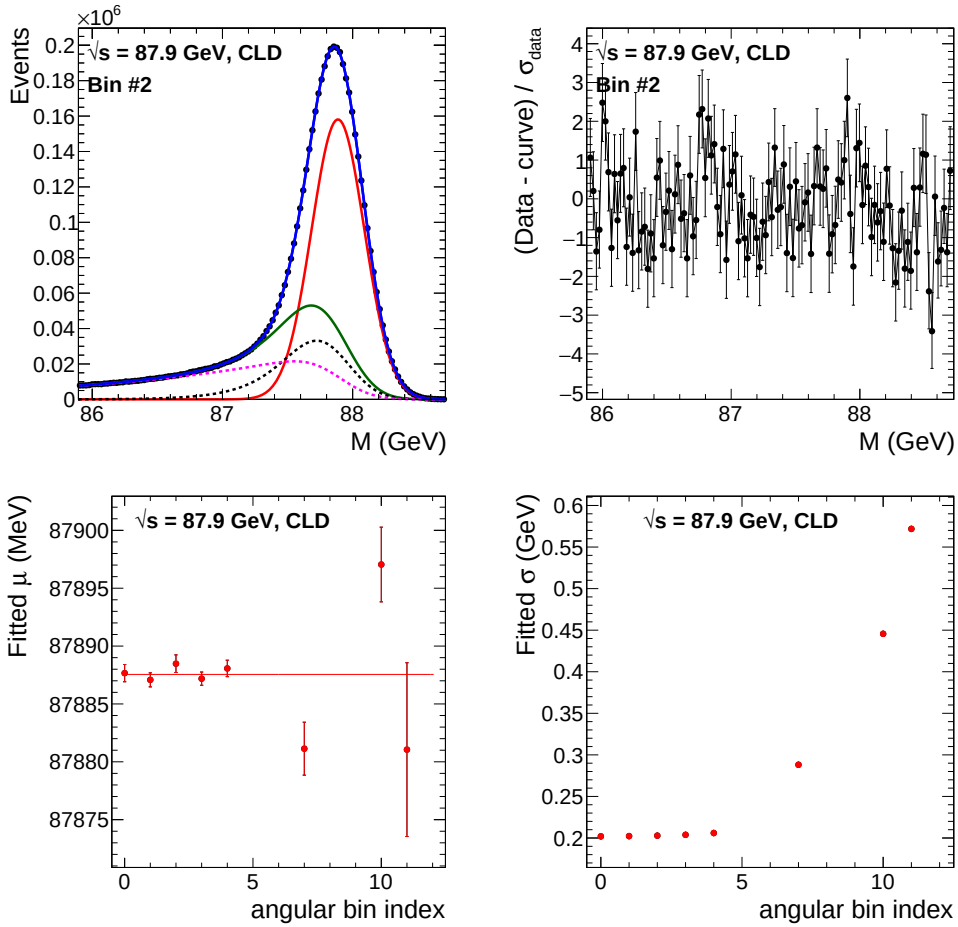

Fig. 5: Same as Figure 3, but using the reconstructed mass in the CLD detector at $\sqrt{s} = 87.9$ GeV.

Breit-Wigner with the Gaussian function that describes the BES. In the right panel of Fig.7, the red symbols show again the biases obtained from the IDEA samples, but shifted by a constant amount, such that the bias is zero at 87.9 GeV by convention. The curve of Fig. 2, resulting from maximising the product of the Z Breit-Wigner with the Gaussian describing the BES, is now overlaid, shifted as well such that it crosses the origin at $\sqrt{s} = 87.9$ GeV. This overlay confirms the similarity of the two shapes. On this shifted y-scale, the knowledge of Δb boils down to the precision with which the point at $\sqrt{s} = 94.3$ GeV can be predicted. In the same plot, the black open symbols show the (shifted) biases obtained from the Monte-Carlo samples, when the generator-level invariant mass is fitted instead of the reconstructed mass. Hence, the black symbols and the full curve both include no detector effect. The former result from the state-of-the-art modelling of radiation effects as implemented in the Monte-Carlo program, while the latter is obtained from a very simple model with no radiation at all. At 94.3 GeV, the difference between these two predictions amounts to 500 keV. Consequently, if the ISR and FSR effects are known to 1% (5%) for example, which is probably within reach, Δb would be known to 5 keV (25 keV). Similarly, the comparison between the black and the red symbols shows the sole effect of the detector response. It shows that it will be sufficient to model the detector effects at the level of a few percent to ensure that the corresponding uncertainty on Δb is small compared to the statistical uncertainty of the first term in Equation 4.

Consequently, in Equation 4, the uncertainty of the second term can be neglected, and the point-to-point uncertainty on $\sqrt{s}$ is given by the statistical uncertainty of the first term. As mentioned above, this uncertainty amounts to 28 keV with the resolution of the IDEA detector (and to about 58 keV with the CLD detector). The corresponding systematic

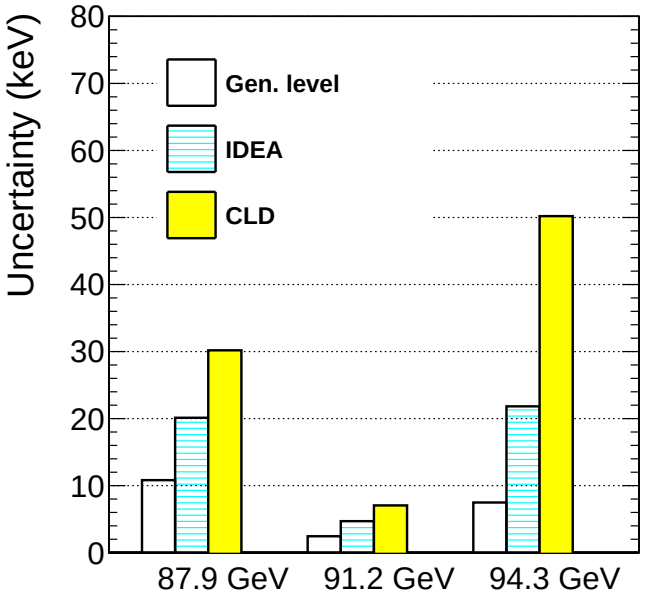

Fig. 6: Statistical uncertainty in the estimator of $\sqrt{s}$ extracted from fits to the measured dimuon invariant mass distribution, expected with the full FCC-ee event sample of the Z lineshape scan (125 ab^{-1} at the Z peak and 40 ab^{-1} at each off-peak energy). This uncertainty is shown assuming an ideal detector resolution (leftmost bars), the resolution of the IDEA detector (middle bars), and that of the CLD tracker (rightmost bars).

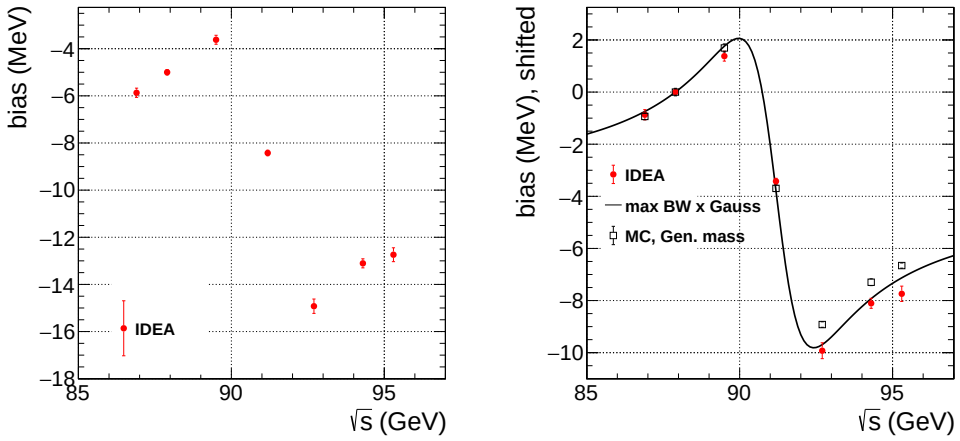

Fig. 7: Left: The difference (bias) between the $\sqrt{s}$ extracted from the dimuon invariant mass fit and the true value, as a function of $\sqrt{s}$. The resolution of the IDEA detector is assumed. Right: The biases are shown for the simulated performance of the IDEA detector (red points) and for the dependence that would be expected with a perfect detector, including (open black symbols) or not (black curve) ISR/FSR effects. An overall, energy independent offset of a few MeV has been subtracted, so that the bias is zero at 87.9 GeV, for all sets of points.

uncertainty on the Z width follows from [9]:

$$\delta\Gamma_Z \simeq \frac{\Gamma_Z}{\sqrt{s}_+ - \sqrt{s}_-} \times \delta(\sqrt{s}_+ - \sqrt{s}_-) \quad , \tag{5}$$

which leads to $\delta\Gamma_Z \simeq 11$ keV with the resolution of the IDEA detector.

Achieving the 20 keV uncertainty shown in Fig. 6 requires that the momentum scale (in particular the B field) be stable to the level of 2×10^{-7} (20 keV over 91 GeV) – or at least, that the variations of the scale be monitored to that level. Such a level of monitoring may be difficult to achieve with usual NMR field probes, but can be achieved in situ using low mass resonances, as will be shown in the next section.

3 Stability of the track momentum scale

To monitor the stability of the track momentum scale, a first idea could be to use J/ψ mesons (which are mostly produced in Z to $b\bar{b}$ events) in their decays to muons. The production rate of events containing a $J/\psi \to \mu\mu$ is smaller than the production rate of $Z \to \mu\mu$ events by a factor of 150, but the mass resolution of the J/ψ's is much better than that of $Z \to \mu\mu$ decays. A Monte-Carlo sample of hadronic Z decays has been used to study this resolution. After fitting the two muon tracks to a common vertex, the dimuon invariant mass is obtained from the tracks' momenta at this vertex, and the resulting resolution is of typically 2 MeV with the IDEA detector. The precision with which the position of the J/ψ mass peak could be determined, in 40 ab^{-1} at 87.9 GeV (this energy being chosen since that is where the Z cross-section is lowest), can be estimated from a simple scaling of what was obtained previously:

$$30\,\text{keV} \quad \times \sqrt{10^7/8.9\,10^9} \quad \times \sqrt{150} \quad \times \frac{2\,\text{MeV}}{90\,\text{MeV}} \quad = \quad 0.28\,\text{keV} \tag{6}$$

In Eq. 6, the first term (30 keV) is the precision with which the $Z \to \mu\mu$ peak can be reconstructed in 10^7 non-radiative events (see Fig. 1); the product of the two square roots rescales this precision to the expected number of $J/\psi \to \mu\mu$ decays; the resulting precision is finally multiplied by the ratio of the mass resolutions seen in the two decays. The result corresponds to a relative precision of 9×10^{-8} on the position of the J/ψ mass peak. To assess the stability of the momentum scale, the full dataset at 87.9 GeV could be split into, for example, 100 subsamples in time (one subsample would then correspond to typically one day of data taking). By looking at the variations of the position of the J/ψ mass peak in these subsamples, the scale stability would be monitored to 9×10^{-7}, which is four times larger than the target precision.

Instead, the decays of K_s into charged pions can be exploited. With roughly one such decay in every second hadronic Z event, the statistics is enormous. The reconstruction of such K_s decays has been studied in a Monte-Carlo sample of hadronic Z decays and follows the algorithm presented in Ref. [10]. It starts with the identification of the "primary tracks", that can be fit to a primary vertex[2], and, consequently, of the "secondary tracks". Moreover, all reconstructed particles are used to determine the thrust axis, and the plane orthogonal to this axis and containing the interaction point divides each event in two hemispheres. Pairs of opposite-charge secondary tracks that belong to a same hemisphere are fit to a common vertex. Pairs for which the vertex fit has a good χ^2 (a rather loose cut, $\chi^2 < 10$, being used here), and whose invariant mass (determined from the tracks' momenta at the fitted vertex) is consistent with the K_s mass, define $K_s \to \pi^+\pi^-$ candidates. Figure 8 shows the mass distribution of such K_s candidates obtained in a Monte-Carlo sample of hadronic Z decays, modelling the response of the IDEA detector. The distribution is shown on purpose in a wide mass range, in order to show that the background is low.

To determine the precision with which the position of the $K_s \to \pi^+\pi^-$ mass peak can be determined, the mass distribution of the K_s candidates in the $Z \to$ hadrons Monte-Carlo sample (which corresponds to a luminosity of 2 fb^{-1}) has been fitted by the sum of three Gaussian functions that share the same mean, plus a constant term to account for the background. The fits have been made in bins of polar angle (similarly to what was done in Section 2.2), and of the momentum of each leg, resulting in a three-dimensional binning.

[2] A simple iterative algorithm is used here. In a first step, all tracks are fit to a common vertex, using a constraint given by the beam-spot size. The track that gives the largest contribution to the χ^2 of the fit is removed, and the remaining tracks are fit again. The procedure is repeated until the χ^2 contribution of each track is below a given cut.

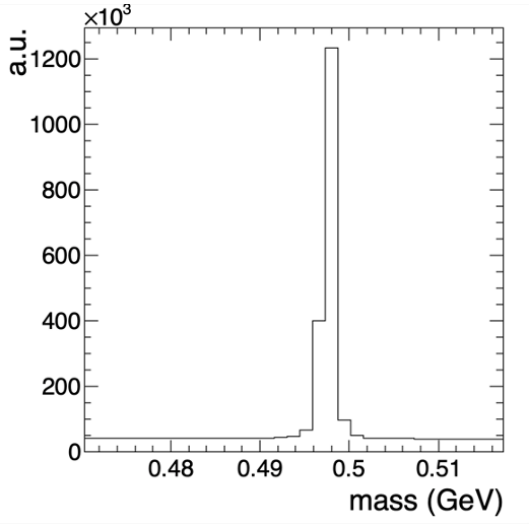

Fig. 8: Distribution of the mass of $K_s \to \pi^+\pi^-$ candidates in a Monte-Carlo sample of hadronic Z decays, modelling the response of the IDEA detector.

The momentum bins correspond to $0.5 < p < 2$ GeV, $2 < p < 5$ GeV, and $p > 5$ GeV.

An example fit is shown in Fig. 9, for a forward angular bin and when both pions have more than 5 GeV of momentum. The fit quality is acceptable. Figure 10 shows the common

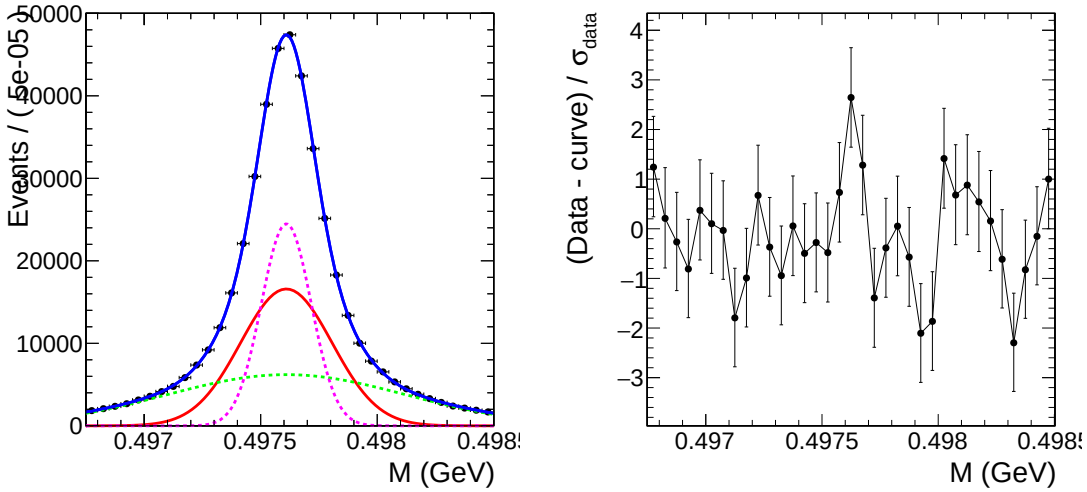

Fig. 9: Example fit of the mass distribution of K_s candidates (left) and the corresponding pulls (right). The resolution of the IDEA detector is assumed. The three Gaussian functions that enter in the fit model are shown separately as the red, magenta and green curves.

mean of the three Gaussians, resulting from the fits made in the various kinematic bins. Within the uncertainties, the fitted mean is consistent across all the bins, and the position of the K_s mass peak is taken to be the weighted average of all these measurements. With the statistics of the Monte-Carlo sample used here, the uncertainty of this weighted average amounts to 0.05 keV. Rescaling to an integrated luminosity of 40 ab^{-1} at 87.9 GeV leads to a relative uncertainty of 3×10^{-9} on the position of the K_s mass peak. Hence, splitting the dataset into 100 subsamples would allow the stability of the momentum scale to be monitored to 3×10^{-8}. The monitoring can thus be performed to the desired level. An increased granularity could even be contemplated, for example by splitting the subsamples into about 50 angular bins.

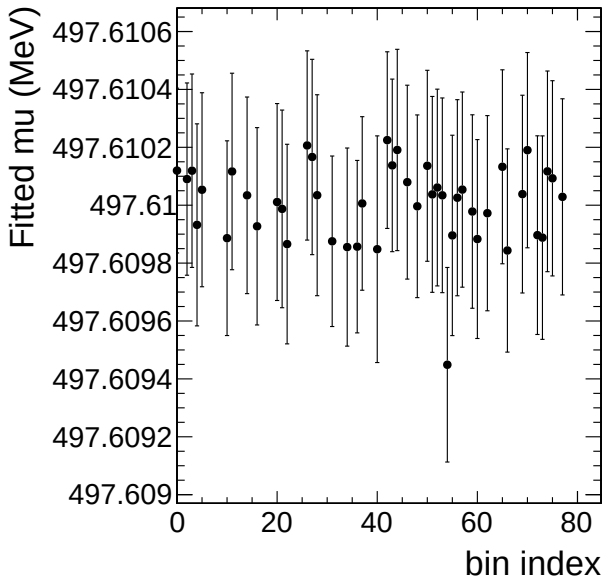

Fig. 10: Common mean of the three Gaussian functions obtained from the fits of the K_s mass distribution made in the various kinematic bins.

A study to assess whether this level of monitoring could also be achieved using decays of Φ mesons into two charged kaons, such that the monitoring would use prompt instead of displaced tracks, is under way.

4 Conclusions

The statistics expected at FCC-ee, together with the excellent track momentum resolution of the IDEA drift chamber, offer the potential to control the point-to-point systematic uncertainty on the centre-of-mass energy, in the Z lineshape scan, to about 28 keV (about 58 keV with the resolution of the CLD detector). This uncertainty translates into a 11 keV uncertainty on the Z width, which goes up to 12 keV when adding in quadrature the subleading uncertainty arising from the knowledge of the beam energy spread [11]. Reaching this precision requires that the track momentum scale be stable at the level of 2×10^{-7}. With the IDEA tracker, the monitoring of the position of the K_s mass peak, measured in the decays of K_s mesons into charged pions, will allow the stability of the scale to be controlled to that unprecedented level, thanks to the excellent track momentum resolution of the IDEA drift chamber for soft tracks.

The statistical uncertainty of the Z width will be only three times lower than the aforementioned systematic uncertainty. We are thus approaching the regime where the measurement of the Z width will not be limited by systematic uncertainties related to $\sqrt{s}$ measurements. Other sources of systematic uncertainties which, at LEP, had been negligible, now have to be revisited. In particular, the relative uncertainty of the luminosity determination between the energy points used in the scan will have to be controlled to 10^{-5} or better, in order to lead to a systematic uncertainty that is smaller than the $\sqrt{s}$ related uncertainty.

References

[1] A. Blondel, et al., Polarization and Centre-of-mass Energy Calibration at FCC-ee (2019). arXiv:1909.12245 [physics.acc-ph]

[2] The IDEA Study Group, The IDEA detector concept for FCC-ee (2025). URL https://arxiv.org/abs/2502.21223. arXiv:2502.21223 [physics.ins-det]

[3] N. Bacchetta, et al., CLD – A Detector Concept for the FCC-ee (2019). arXiv:1911.12230 [physics.ins-det]

[4] A. Arbuzov, S. Jadach, Z. Was, B.F.L. Ward, S.A. Yost, The Monte Carlo Program KKMC , for the Lepton or Quark Pair Production at LEP/SLC Energies—Updates of electroweak calculations. Comput. Phys. Commun. **260**, 107734 (2021). https://doi.org/10.1016/j.cpc.2020.107734. arXiv:2007.07964 [hep-ph]

[5] W. Kilian, T. Ohl, J. Reuter, WHIZARD: Simulating Multi-Particle Processes at LHC and ILC. Eur. Phys. J. C **71**, 1742 (2011). https://doi.org/10.1140/epjc/s10052-011-1742-y. arXiv:0708.4233 [hep-ph]

[6] de Favereau, J. and Delaere, C. and Demin, P. and Giammanco, A. and Lemaître, V. and Mertens, A. and Selvaggi, M., DELPHES 3, A modular framework for fast simulation of a generic collider experiment. JHEP **02**, 057 (2014). https://doi.org/10.1007/JHEP02(2014)057. arXiv:1307.6346 [hep-ex]

[7] B. Madison, G.W. Wilson, Center-of-mass energy determination using $e^+e^- \to \mu^+\mu^-(\gamma)$ events at future e^+e^- colliders (2022). arXiv:2209.03281 [hep-ex]

[8] W. Verkerke, D.P. Kirkby, The RooFit toolkit for data modeling. eConf **C0303241**, MOLT007 (2003). arXiv:physics/0306116

[9] S. Schael, et al., Precision electroweak measurements on the Z resonance. Phys. Rept. **427**, 257–454 (2006). https://doi.org/10.1016/j.physrep.2005.12.006. arXiv:hep-ex/0509008

[10] R. Aleksan, L. Oliver, E. Perez, CP violation and determination of the bs flat unitarity triangle at an FCC-ee. Phys. Rev. D **105**(5), 053008 (2022). https://doi.org/10.1103/PhysRevD.105.053008. arXiv:2107.02002 [hep-ph]

[11] FCC Feasibility Study Report (2025).